ScienceDirect®

Original Research Article

LC and LC–MS/MS studies for the identification and characterization of degradation products of acebutolol

Uday Rakibe [a], Ravi Tiwari [b] 👤 ✉ , Anand Mahajan [c], Vipul Rane [a], Pravin Wakte [a]

Show more ⌄

≔ Outline | ⌷ Share   🗩 Cite

Get rights and content ↗

Abstract

The aim of the present investigation was to demonstrate an approach involving use of liquid chromatography (LC) and liquid chromatography-mass spectrometry (LC–MS) to separate, identify and characterize very small quantities of degradation products (DPs) of acebutolol without their isolation from the reaction mixtures. The drug was subjected to oxidative, hydrolytic, thermal and photolytic stress conditions as per International Conference on Harmonization (ICH) guideline Q1A(R2). Among all the stress conditions the drug was found to be labile in hydrolytic (acidic & basic) and photolytic stress conditions, while it was stable in water-induced hydrolysis, oxidative and thermal stress conditions. A total of four degradation products were formed. A C_{18} column was employed for the separation of all the DPs on a gradient mode by using high-performance liquid chromatography (HPLC). All the DPs were characterized with the help of their fragmentation pattern and the masses obtained upon LC–MS/MS and MS^n analysis. All the hitherto unknown degradation products were identified as 1-(2-(2-hydroxy-3-(isopropylamino)propoxy)-5-(amino)phenyl)ethanone (DP-I), N-(4-(2-hydroxy-3-(isopropylamino)propoxy)-3-acetylphenyl)acrylamide (DP-II), 1-(2-(2-hydroxy-3-(isopropylamino)propoxy)-5-(hydroxymethylamino)phenyl)ethanone (DP-III) and 1-(6-(2-hydroxy-3-(isopropylamino)propoxy)-2,3-dihydro-2-propylbenzo[d]oxazol-5-yl)ethanone (DP-IV). Finally the

in-silico carcinogenicity and hepatotoxicity predictions of the drug and all the DPs were performed by using toxicity prediction softwares viz., TOPKAT, LAZAR and Discovery Studio ADMET. The results of in-silico toxicity studies revealed that acebutolol (0.967) and DP-I (0.986) were found to be carcinogenic, while acebutolol (0.490) and DP-IV (0.437) were found to be hepatotoxic.

Keywords

Acebutolol; Stress testing; LC; LC–MS/MS; Degradation pathway; In-silico toxicity

1. Introduction

Acebutolol hydrochloride is a selective, hydrophilic beta-adrenoreceptor blocker which is used to treat hypertension and ventricular arrhythmias. Other beta-adrenergic agents are atenolol, betaxolol, celiprolol, bisoprolol, esmolol, metoprolol, nebivolol, etc. Chemically acebutolol (Fig. 1) is N-[3-Acetyl–4-[2–hydroxy–3-[(1–methylethyl)amino]propoxy]-butanamide [1]. There exist various reports on investigation and analysis of acebutolol by using different analytical techniques such as high-performance liquid chromatography (HPLC), thin layer chromatography, ion pair HPLC, liquid chromatography with tandem mass spectrometry (LC–MS/MS), voltammetry, and polarography. The drug is reported for the enantioselective determination of its active metabolite diacetolol in spiked human plasma samples by LC–MS/MS [2], [3], [4], [5], [6], determination in pharmaceutical formulations and biological fluids by voltammetric method [7], and major metabolite determination in infant's blood circulation and breast milk by a stereospecific HPLC assay method [8]. There are HPLC methods reported for acebutolol doping analysis and toxicological investigations of fatal cases of acebutolol self-poisoning [9], [10]. A literature report is also available on comparative HPLC and LC–MS analysis of antiepileptic with beta-blocking drugs [11]. Acebutolol is also explored by ion-pair HPLC method for its determination in pharmaceuticals [12]. However, very few reports are on acebutolol stability studies and its determination in acid induced degradation products (DPs) and identification of radiodegradation products by irradiation of high dose ionizing radiation emitted by beam of high energy electrons [13], [14], [15].
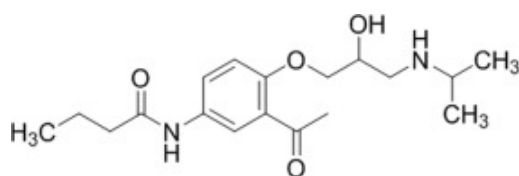
Download : Download high-res image (42KB)
Download : Download full-size image

Fig. 1. Structure of acebutolol.

Hence, the endeavor of the present study was to separate, identify and characterize DPs of acebutolol formed under ICH Q1A(R2) [16] recommended stress conditions of hydrolysis (acid, base and neutral), oxidation, dry heat and photolysis. Moreover, the parallel objective of this study was to explore comprehensive information on the degradation pathway of the drug. To achieve this task a systematic outline of the study includes (i) degradation study of acebutolol under conditions of oxidation, hydrolysis, thermal and photolysis, (ii) separation of DPs and validation of the developed LC method, (iii) characterization of DPs by LC–MS/MS and MS^n studies, (iv) proposal of degradation pathway of the drug, and (v) prediction of in-silico carcinogenicity and hepatotoxicity of the drug and DPs by different models.

2. Experimental

2.1. Drug and reagents

Pure acebutolol was purchased from Sigma-Aldrich (Mumbai, India). Analytical reagent (AR) grade sodium hydroxide (NaOH), ammonium formate (NH_4HCO_2), formic acid (HCOOH) and HPLC grade methanol were purchased from Merck Specialities Pvt. Ltd. (Mumbai, India). AR grade hydrochloric acid (HCl) and 30% hydrogen peroxide were purchased from Qualigens Fine Chemicals Pvt. Ltd. (Mumbai, India) and S.D. Fine-Chem. Ltd. (Mumbai, India), respectively. Ultra-pure double distilled HPLC grade water obtained from Labsil Instruments (Bangalore, India) was used throughout the studies.

2.2. Equipments

An HPLC system (Shimadzu Corporation, SPD-M20A, Kyoto, Japan) equipped with LC Solution software was used for LC studies equipped with a photo-diode array (PDA) detector, sample injector with 20 µL loop, and on-line degasser containing binary pump. The output signals were assessed on a Dell computer using LC Solution software. Stress degradation studies were carried out using precision water bath (Meta-Lab Ltd., Mumbai, India) containing a thermostat for temperature control. A hot air oven (Scientico Ltd., Mumbai, India) was used to perform solid state thermal stress studies. Photodegradation studies were executed in a photostability chamber (Thermolab Scientific Equipments Pvt. Ltd., Mumbai, India), where the temperature was adjusted to 25 ± 2 °C during the study. The measurement of visible and near UV illumination energy was carried out by using a calibrated lux and UV meter (Thermolab Scientific Equipments Pvt. Ltd., Mumbai, India) [17]. The LC–MS system controlled by Xcalibur software (version 2.0) consisted of LCQ Fleet and TSQ Quantum Access with Surveyor Plus HPLC System (Thermo, San Jose, USA). All the separation studies were carried out using a C_{18} column (150 mm × 4.6 mm i.d., particle size 5 µm) Kromasil (Eka Chemicals AB, Bohus, Sweden). A pH meter (Controlled Dynamics, Vadodara, India) was used to adjust the pH of mobile phase and all other solutions used during the study. Other equipments used

during the study were weighing balance (Shimadzu, AUX220, Kyoto, Japan), sonicator (Spectralab UCB 30, Mumbai, India) and analytical balance (Precissa XR 205 SMDR, Moosmattstrasse Dietikon, Switzerland).

2.3. Forced degradation studies

The objective of forced degradation studies was to achieve 10%–15% degradation of the drug. The drug was subjected to oxidative, hydrolytic, thermal and photolytic stresses. The results were obtained by comparing four samples of every stress condition viz., untreated blank sample, stressed blank sample, untreated standard drug sample and stressed drug sample solution. In case of thermal and photolytic stress conditions only two samples were generated viz., sample exposed to stress condition and control sample.

2.3.1. Hydrolytic degradation

The hydrolytic decomposition was performed in acidic, alkaline and neutral conditions. Samples were prepared by taking 1 mL of stock solution of drug (1000 μg/mL) and 1 mL of hydrolytic agent (1 M HCl, 1 M NaOH and water) in 10 mL volumetric flask. If required, the samples were heated at constant temperature on water bath at 80 °C for specified time intervals. The samples were neutralized by using equal strength of acid or alkali before injected into HPLC system.

2.3.2. Oxidative degradation

Oxidative degradation was carried out by using hydrogen peroxide. Samples were prepared by taking 1 mL of stock solution of the drug (1000 μg/mL) and 1 mL of hydrogen peroxide (30%) in 10 mL volumetric flask. If required, the samples were heated on constant temperature water bath at 80 °C for specified time intervals. After required exposure samples were diluted up to the mark by using diluent and subjected for HPLC analysis.

2.3.3. Thermal degradation

Drug sample of 10 mg each was taken in two 10 mL volumetric flasks and sealed. One flask was exposed to dry heat in hot air oven for specified temperature and time interval and the other was kept as control. After required exposure two separate solutions were prepared by weighing appropriate amounts of the sample exposed to thermal stress and control to produce concentration of 100 μg/mL. The samples were diluted up to the mark with the help of diluent and injected separately into HPLC.

2.3.4. Photodegradation

The drug layer of 1 mm thickness was prepared in a petri dish and exposed to ICH recommended photostability conditions with the overall illumination of not less than 1.2 million lx h along with the integrated near ultraviolet energy of not less than 200 W h/m². Another petri dish containing the drug (1 mm layer thickness) was wrapped with aluminum foil and kept as control. After

required exposure two separate solutions were prepared by weighing appropriate amounts of the sample exposed to stress and control to produce concentration of 100 μg/mL. The samples were diluted up to the mark with the help of diluent and injected separately into HPLC.

Photodegradation of the drug was also carried out in solution phase. Two solutions with the concentration of 100 μg/mL were prepared in 10 mL volumetric flask by using methanol as diluent. One was exposed to ICH dose of light and the other was kept as control.

2.4. HPLC method development

HPLC studies were carried out individually on all the reaction solutions and then on the mixture of those solution in which the degradation was observed. A duplicate sample of each stress condition was injected into HPLC system along with a separate blank stress sample to achieve an optimum degradation. To accomplish an appropriate separation and to resolve all the polar DPs overlapping/ merging, various HPLC trials were conducted. The separation was executed using different proportions of acetonitrile (ACN), methanol (MeOH) and ammonium formate buffer (10 mM) by varying the pH of buffer with formic acid. The detection wavelength, injection volume and flow rate were 235 nm, 20 μL and 1 mL/min, respectively.

2.5. HPLC method validation

The developed LC method was validated by covering various parameters outlined in the ICH guidelines Q2(R1) [18]. The selected validation parameters included linearity, precision (inter-day and intra-day), accuracy, specificity, and selectivity.

2.5.1. Linearity

Linearity of the method was established by using solutions containing 50–250 μg/mL of the drug. Each linearity sample was injected in triplicate into the HPLC column by keeping the injection volume constant.

2.5.2. Precision

A precision study was carried out by injecting the drug with three different concentrations (100, 150 and 200 μg/mL) in triplicate into the HPLC on the same day and the next day. The values of standard deviation (SD) and percent relative standard deviation (% RSD) were calculated for both intra-day and inter-day precision.

2.5.3. Accuracy

The accuracy of the method was established by conducting recovery studies of pure drug from degradation samples by standard addition method. The mixtures of stressed samples were spiked with the drug with concentrations of 80, 120 and 160 μg/mL.

2.5.4. Specificity and selectivity

The specificity of the method was investigated through establishment of resolution factor between the drug peak and the nearest resolving peak, and also among other peaks. Selectivity was confirmed through peak purity studies using a PDA detector. A mixture of degradant was produced by mixing an equal amount of solutions generated during different stress conditions and subjected for HPLC analysis.

2.6. Mass spectral studies on the drug

Mass spectral studies were performed in positive electrospray ionization (ESI) mode in the mass range of 50–1000 Da to establish the fragmentation pattern of the drug. In order to get clear mass spectrum without any background noise, the drug at a concentration of 5 μg/mL in methanol:water (50:50, v/v) was directly infused using a syringe pump into the mass spectrometer. The mass parameters were appropriately tuned to get clear molecular ion peak of the drug. High purity nitrogen was used as the nebulizer and auxiliary gas. The drug was further subjected to MS/MS analysis in positive ESI mode to explore the origin of each individual fragment.

2.7. LC–MS/MS studies

The degraded drug samples were subjected to LC–MS/MS analysis in positive ESI mode using the previously developed gradient LC method. A satisfactory separation of degradation products was achieved by using C_{18} column. For structure elucidation of the DPs, the samples with maximum degradation were subjected to LC–MS analysis. The structural identity of each DP was performed with the LC–MS fragmentation analysis.

2.8. In-silico toxicity studies

The drug and all its degradation products were subjected to in-silico carcinogenicity and hepatotoxicity predictions by using different models. Carcinogenicity prediction was performed by using Toxicity Prediction by Komputer Assisted Technology (TOPKAT) version 6.2, Lazar Toxicity Prediction software version 1.1.2 building on top of the OpenTox framework and adopting DSSTox database, TOPKAT Extensible built with Bayesian models and partial least square (PLS) technique. Hepatotoxicity prediction was carried out by using Discovery Studio ADMET. The model was developed from available literature data of 382 compounds known to exhibit liver toxicity or trigger dose-related elevated aminotransferase levels in more than 10% of the human population [19].

3. Results and discussion

3.1. Degradation behaviour

The chromatogram in Fig. 2 reveals the degradation behaviour of acebutolol. A total of four degradation products were generated from the drug (denoted as I-IV according to the elution order

in the chromatogram). A major degradation product (DP-I) was formed in both acid and alkaline stress conditions, while the other major degradation product (DP-IV) was generated only in alkaline stress condition. Two minor degradation products, DP-II and DP-III, were formed only in photolytic stress condition. This shows that the acebutolol is photo labile to a certain extent and an indication for the bulk drug substance and generic drug product manufacturers to optimize the critical quality attributes (CQA) to avoid the significant light exposure during the manufacturing process. Apart from the above listed stress conditions the drug was found to be stable in neutral (heating in water), oxidative and thermal stress conditions.
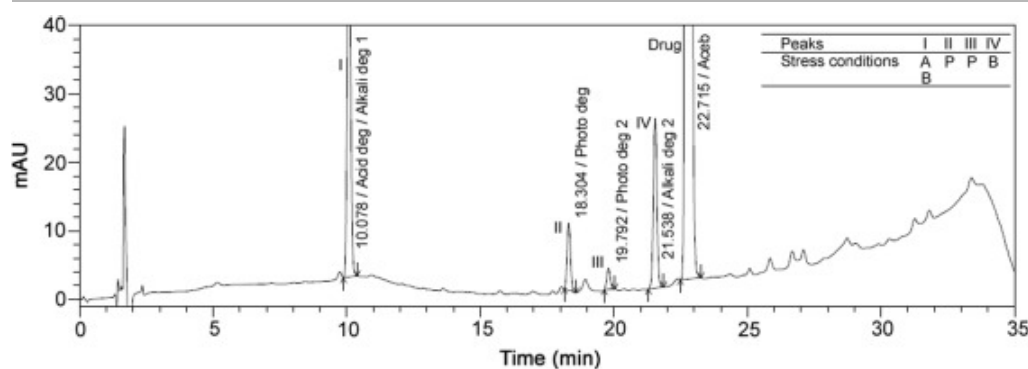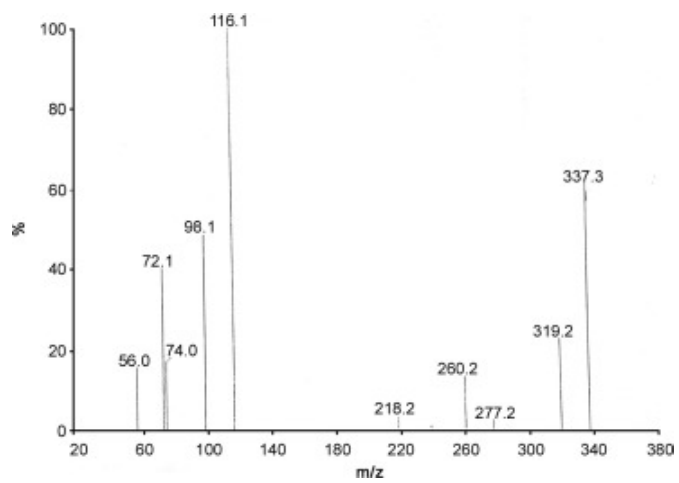

Download : Download high-res image (144KB)
Download : Download full-size image

Fig. 2. HPLC chromatogram of all the acebutolol products (I-IV) and acebutolol.
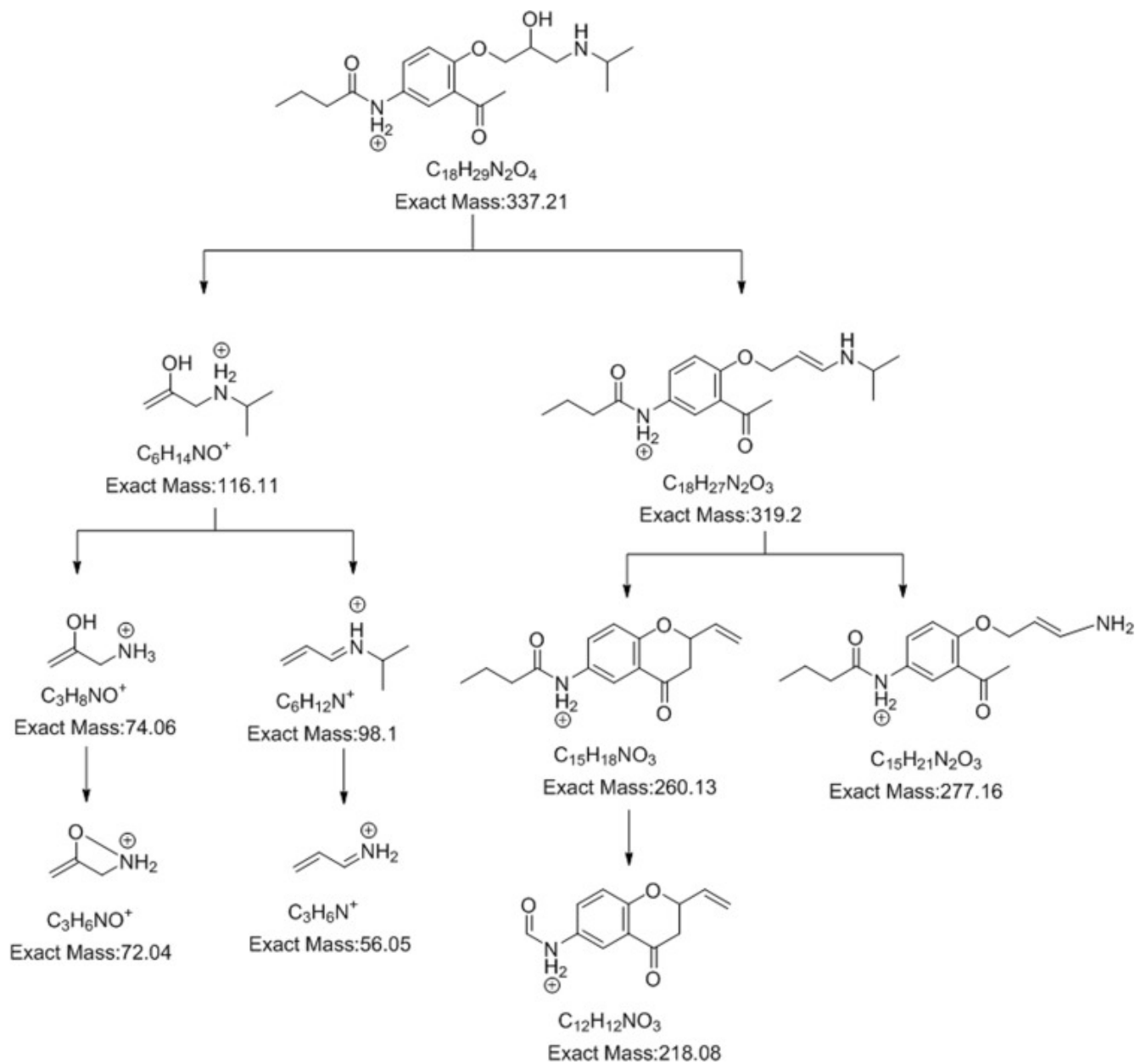
3.2. Fragmentation pathway of the drug

As shown in Fig. 3, a total of 10 fragments were formed from the drug. Molecular ion fragment of the drug (numbered as 0) had the mass of 337.21, which followed a parallel fragmentation pathway. The two fragments of m/z 116.11 and m/z 319.20 were formed from the drug due to the cleavage of ether linkage of the side chain and loss of hydroxyl group, respectively (Fig. 4). Two types of fragment ions can be easily identified in Fig. 4, viz., side chain fragment ions and cyclic structure fragment ions. The fragment with m/z 116.11 on loss of isopropyl resulted in ion with m/z 74.06, in which lone pair of electrons of nitrogen succeeded in cyclic structure (m/z 72.04) formation with the terminal hydroxyl group. In the alternate fragmentation pathway of ion with m/z 116.11, the ions with m/z 98.10 and m/z 56.05 were formed on loss of hydroxyl and isopropyl groups, respectively. In this fragmentation part, the bond cleavages took place between carbon and heteroatom linkages, which are considered to be loose links as compared to C–C bond. On the other hand, the fragment with m/z 319.20 was formed from the drug on loss of hydroxyl group, and then in the subsequent step the fragment with m/z 319.20 underwent cleavage of isopropyl amine and isopropyl entities from the terminal side chain to form a cyclic fragment ion with m/z 260.13 and m/z 277.16, respectively. Finally, the fragment with m/z 260.13 on loss of a propyl group from the side chain led to the ion with m/z 218.08. The interpretation of MS/MS data of fragments of the drug is shown in Table 1, and the complete fragmentation pathway of the drug is shown in Fig. 4.

Download : Download high-res image (100KB)

Download : Download full-size image

Fig. 3. Line spectrum of acebutolol obtained in MS study.

Download : Download high-res image (385KB)

Download : Download full-size image

Fig. 4. Fragmentation pathway of acebutolol.

Table 1. Interpretation of MS/MS data of fragments of acebutolol.

Peak no.	Experimental mass	Best possible molecular formulae	Theoretical mass	RDB [a]	Possible parent fragment	Difference from parent ion	Possible losses corresponding to difference
0	337.30	$C_{18}H_{29}N_2O_4^+$	337.21	5.5			
1	319.20	$C_{18}H_{27}N_2O_3^+$	319.20	6.5	0	18.00	H_2O

Peak no.	Experimental mass	Best possible molecular formulae	Theoretical mass	RDB [a]	Possible parent fragment	Difference from parent ion	Possible losses corresponding to difference
2	277.20	$C_{15}H_{21}N_2O_3^+$	277.16	6.5	1	42.04	C_3H_6
3	260.20	$C_{15}H_{18}NO_3^+$	260.13	7.5	1	59.04	C_3H_9N
4	218.20	$C_{12}H_{12}NO_3^+$	222.11	6.5	3	42.08	C_3H_6
5	116.10	$C_6H_{14}NO^+$	116.11	0.5	0	220.97	$C_{12}H_{15}NO_3$
6	98.10	$C_6H_{12}N^+$	98.10	1.5	5	18.14	H_2O
7	74.00	$C_3H_8NO^+$	74.06	0.5	6	42.05	C_3H_6
8	72.10	$C_3H_8NO^+$	72.04	1.5	7	2.20	H_2
9	56.00	$C_3H_6N^+$	56.05	1.5	8	42.05	C_3H_6

a

RDB: ring plus double bonds.

3.3. LC–MS/MS studies on stressed samples

The mass spectra of all the four degradation products, DP-I-IV, are shown in Fig. 5. The experimental masses, best possible molecular formulae, theoretical mass, RDB (ring plus double bonds) and major fragments of all the DPs are listed in Table 2.
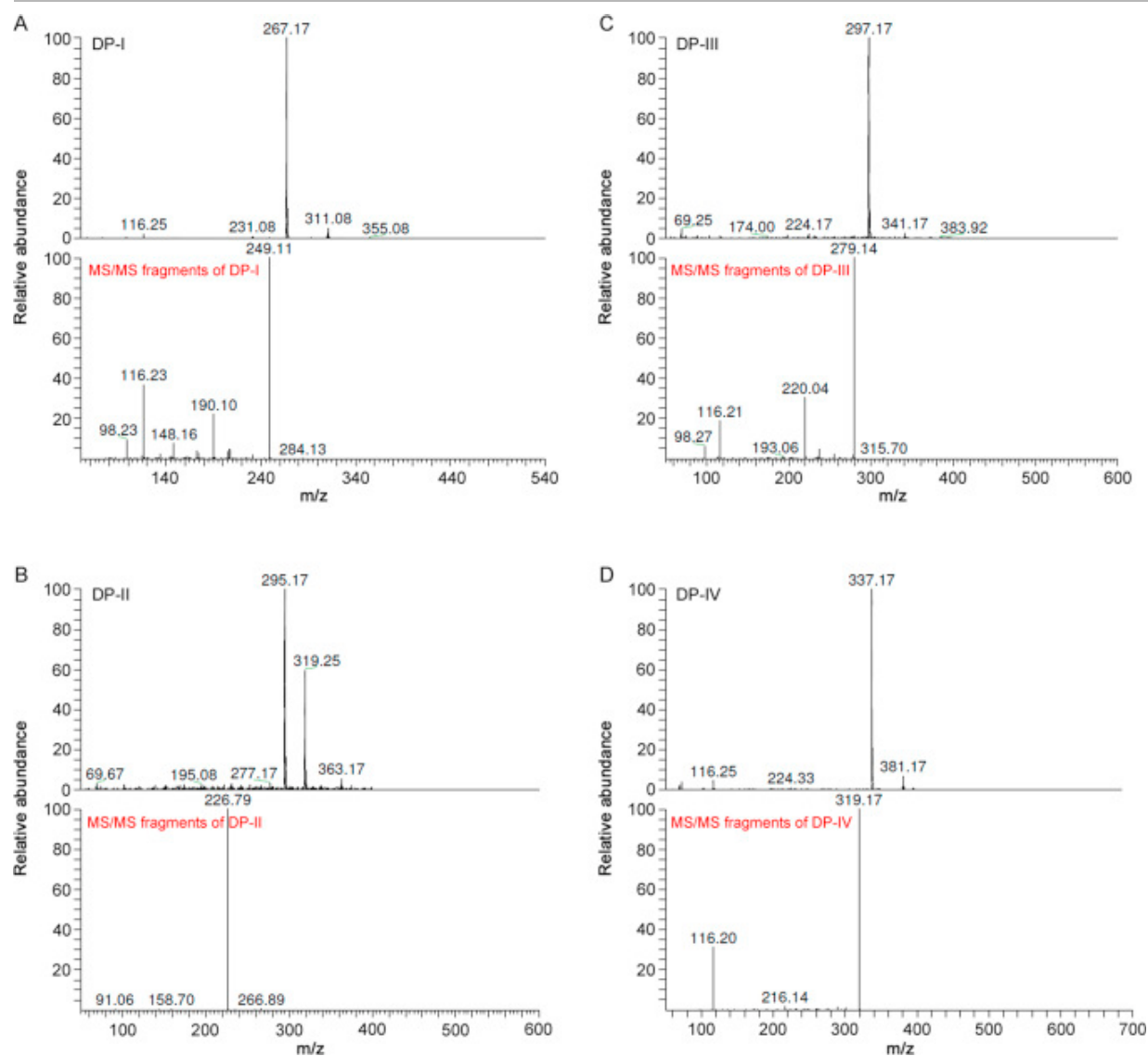
Fig. 5. Line spectra of degradation products: (A) DP-I, (B) DP-II, (C) DP-III and (D) DP-IV obtained in LC–MS/MS studies.

Table 2. LC–MS/MS data of DPs (I-IV) along with their possible molecular formulae and major fragments.

DPs	Experimental mass	Best possible molecular formula	Theoretical mass	RDB [a]	Major fragments (chemical formula)
I	267.17	$C_{14}H_{23}N_2O_3^+$	267.17	4.5	249.11 ($C_{14}H_{21}N_2O_2^+$), 190.10 ($C_{11}H_{12}NO_2^+$), 148.16 ($C_8H_6NO_2^+$), 116.23 ($C_6H_{14}NO^+$), 98.23 ($C_6H_{12}N^+$)

| DPs	Experimental mass	Best possible molecular formula	Theoretical mass	RDB [a]	Major fragments (chemical formula)
II	319.25	$C_{17}H_{23}N_2O_4^+$	319.17	5.5	295.17 ($C_{15}H_{23}N_2O_4^+$), 277.17 ($C_{14}H_{17}N_2O_4^+$), 266.79 ($C_{14}H_{20}NO_4^+$), 226.79 ($C_{11}H_{18}N_2O_3^+$), 195.08 ($C_{11}H_{19}N_2O^+$)
III	297.17	$C_{15}H_{25}N_2O_4^+$	297.18	4.5	279.14 ($C_{15}H_{23}N_2O_3^+$), 224.17 ($C_{11}H_{14}NO_4^+$), 220.04 ($C_{12}H_{14}NO_3^+$), 193.06 ($C_{11}H_{13}O_3^+$)
IV	337.17	$C_{18}H_{29}N_2O_4^+$	337.21	5.5	319.17 ($C_{18}H_{27}N_2O_3^+$), 224.33 ($C_{12}H_{18}NO_3^+$), 216.14 ($C_{12}H_{10}NO_3^+$), 116.20 ($C_6H_{14}NO^+$)

a

   RDB: ring plus double bonds.

3.4. Identification of degradation products

The identification of all the degradation products was achieved with the help of their fragments obtained in LC–MS/MS studies and comparison with fragmentation pattern of the drug obtained in MS/MS and MS^n analysis.

3.4.1. DP-I (m/z 267.17)

As shown in the mass spectrum of DP-I in Fig. 5A, the fragmentation pathway of DP-I was established and the same is shown in Fig. 6. The mass spectrum of DP-I revealed the formation of formate ion adduct with m/z 311.08, which had ~ 44 Da mass units higher than DP-I. This adduct was observed in all the DPs and formed due to ammonium formate mobile phase used during HPLC separation studies. In the initial positive ESI LC–MS analysis of DP-I, a total of three fragments were formed viz., m/z 267.17, 231.08 and 116.25, which could not provid sufficient information about the source of fragment ions. Hence, in the subsequent analysis, ion with m/z 267.17 was fragmented in ion trap MS system, which led to the formation of source ions with m/z 249.11, 190.10, 148.16, 116.23 and 98.23. A similar approach was applied to explore the sources of ions for rest of the DPs. The base peak of fragment with m/z 267.17 (DP-I) was formed as an amide hydrolysis product with the cleavage of butyraldehyde moiety from the drug. The fragment with m/z 267.17 underwent a loss of water molecule and resulted in the formation of ion with m/z 249.11. This ion (m/z 249.11) underwent a parallel pathway and led to the formation of the other two daughter ions of m/z 231.08 and m/z 116.23 on loss of a water molecule and 1-(3-aminophenyl) ethanone, respectively. The ion with m/z 231.08 on loss of ethenamine (C-N cleavage) resulted in daughter ion with m/z 190.10. This parallel pathway was concluded with the loss of an acetyl moiety from ion with m/z 109.10 and led to the formation of daughter ion with m/z 148.16. Finally loss of water molecule from ion with m/z 116.25 resulted in the formation of ion with m/z 98.23.
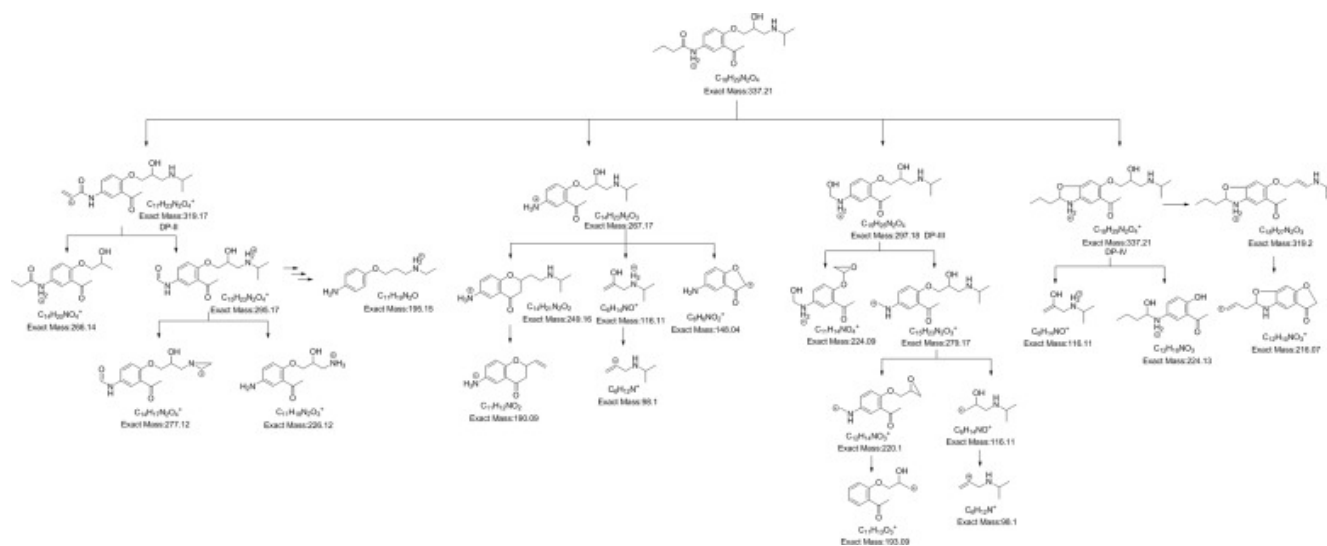
Download : Download high-res image (308KB)

Download : Download full-size image

Fig. 6. Fragmentation pathway of DP-I-IV.

3.4.2. DP-II (m/z 319.17)

As per the mass spectrum of DP-II shown in Fig. 5B, and its fragmentation pattern depicted in Fig. 6, a formation of formate ion adduct with m/z 363.17 was observed which had ~ 44 Da mass units higher than DP-II. Under photolytic conditions as recommended by ICH Q1B, a direct light catalyzed oxidation resulted in loss of a terminal methyl group along with two protons , leading to the formation of DP-II with m/z 319.17. In the subsequent pathway, DP-II resulted in the formation of several daughter ions viz., m/z 295.17, 277.17, 266.89, 226.79, and 195.08. The few remaining ions viz., m/z 158.70, 91.06 and 69.67 might result from background noise; hence they were not considered in the fragmentation pathway. A loss of propan-2-amine and ethene moiety led to the formation of fragments with m/z 266.89 and m/z 295.17, respectively. The fragment with m/z 295.17 on multiple cleavages viz., formaldehyde, water molecule and methyl group led to the formation of ion with m/z 195.08. On the other side, fragment with m/z 277.17 was formed on loss of a methyl group and to compensate this loss, lone pair of electrons of nitrogen underwent cyclization with the terminal methyl to form aziridine ring. The fragment with m/z 226.79 was also formed from m/z 295.17 in a two-step process, which involved an initial loss of methyl group followed by cleavage of isopropyl entity. The proposed structures and fragmentation pathways are outlined in Fig. 6.

3.4.3. DP-III (m/z 297.17)

The mass spectrum of DP-III shown in Fig. 5C, revealed the formation of formate ion adduct with m/z 341.17 which had ~44 Da mass units higher than DP-III. A direct cleavage of propyl group from amide side chain of the drug resulted in the formation of enol form of DP-III with m/z 297.17. DP-III on loss of N-methylpropan-2-amine moiety enabled the newly generating fragment to exhibit

epoxide ring moiety which was evident in the ion fragment with m/z 224.17, while DP-III on loss of water molecule led to the formation of ion fragment with m/z 279.14. There onwards fragments ion (m/z 279.14) followed a parallel pathway of fragmentation with the loss of isopropyl amino group and 1-(2-hydroxy-5-(methylamino) phenyl)ethanone to form daughter ions with m/z 220.04 and m/z 116.21, respectively. A cleavage of methyl amino group from ion fragment m/z 220.04 resulted in ion with m/z 193.06, while loss of water molecule from m/z 116.21 led to the formation of ion with m/z 98.27. The proposed structures and fragmentation pathways are outlined in Fig. 6.

3.4.4. DP-IV (m/z 337.17)

As the line spectra shown in Fig. 5D and fragmentation pathway depicted in Fig. 6 for DP-IV, DP-IV had the mass similar to the drug (m/z 337.21) along with formate ion adduct of ~ 44 Da that other DPs also showed. Based on the similarity of mass, DP-IV was considered as a structural isomer of acebutolol. The side chain carbonyl oxygen underwent cyclization with adjacent phenyl ring to form DP-IV with m/z 337.17. In the subsequent steps, DP-IV on loss of side chain hydroxyl group resulted in the formation of fragment with m/z 319.17 which in the later step led to the loss of N-isopropylprop-1-en-1-amine and resulted in the formation of another cyclic fragment with m/z 216.14. On the other hand, a cleavage on ether linkage of the side chain and loss of 1-(isopropylamino)propan-2-ol from DP-IV led to the formation of ions with m/z 116.25 and 224.33, respectively.

3.5. Method development and validation

The drug and all its degradation products were found to show an acceptable separation by using acetonitrile (A) and ammonium formate buffer (B) (10 mM) with the pH 3.5 in a linear gradient mode (Tmin/A:B: T0/5:95; $T$10/25:75; $T$30/55:45; $T$35/5:95). The LC method validation was performed with respect to the parameters such as linearity, precision, accuracy, specificity and selectivity. In linearity studies, the selected drug concentrations showed an appropriate linear response, and the sensitivity of the method viz., limit of detection (LOD) and limit of quantitation (LOQ), was established from the linearity data. The values of slope and correlation coefficient (r) were 86,347 and 0.998, respectively, whereas the theoretical calculated concentrations for LOD and LOQ were found to be 13.44 μg/mL and 40.74 μg/mL, respectively. The linearity data obtained for the concentrations from 50 μg/mL to 250 μg/mL is shown in Table 3. For inter-day and intra-day precision studies, the % RSD values were 0.73%–1.88% and 0.12%–1.03%, respectively. The accuracy study revealed the percent recovery of the spiked drug in the mixture of stressed samples in the range of 101.07% – 101.58% with the mean recovery of 101.32%. The three known concentrations of the spiked drug were 80, 120 and 160 μg/mL. The developed LC method was found to be specific for each peak with respect to peak purity data obtained using a PDA detector. The relative retention time, peak purity, resolution and single point threshold data of drug and DPs are shown in Table 4. The developed method could be applied to other synthetic small molecules having similar physicochemical properties for the assay, identification and characterization of drug substance and degradation products without their isolation from the reaction mixtures. The developed method

and the characterization technique are suitable for the quantification and identification of acebutolol bulk drug substance containing the degradants/impurities reported in this article.

Table 3. Linearity data for acebutolol.

Conc. (µg/mL)	Injection 1	Injection 2	Injection 3	Average area	Slope	Correlation coefficient (*r*)
50	4,527,102	4,443,534	4,485,356	4,485,331		
100	8,773,153	8,533,928	8,619,327	8,642,136		
150	12,401,889	12,472,518	12,437,144	12,437,184	86,347	0.998
200	17,237,409	17,540,180	17,388,815	17,388,801		
250	21,703,531	21,694,116	21,698,824	21,698,824		

Table 4. Method specificity and peak purity data.

Drug/degradation products	Relative retention time	Peak purity	Single point threshold	Resolution
DP-I	0.227	0.9998	0.9979	0.000
DP-II	0.705	0.9973	0.9924	29.921
DP-III	0.796	0.9960	0.9918	6.031
DP-IV	0.918	0.9994	0.9982	7.909
Acebutolol	1.000	0.9999	0.9999	4.682

3.6. Degradation pathway of the drug

The degradation pathway of the drug under various stress conditions is shown in Fig. 7. DP-I was formed as an amide hydrolysis product on loss of butyraldehyde moiety from the drug, while DP-II was the product obtained on cleavage of acetyl moiety from the drug. DP-III was formed from the drug on loss of propyl group along with a water molecule and DP-IV was obtained as a dehydration product from the drug.
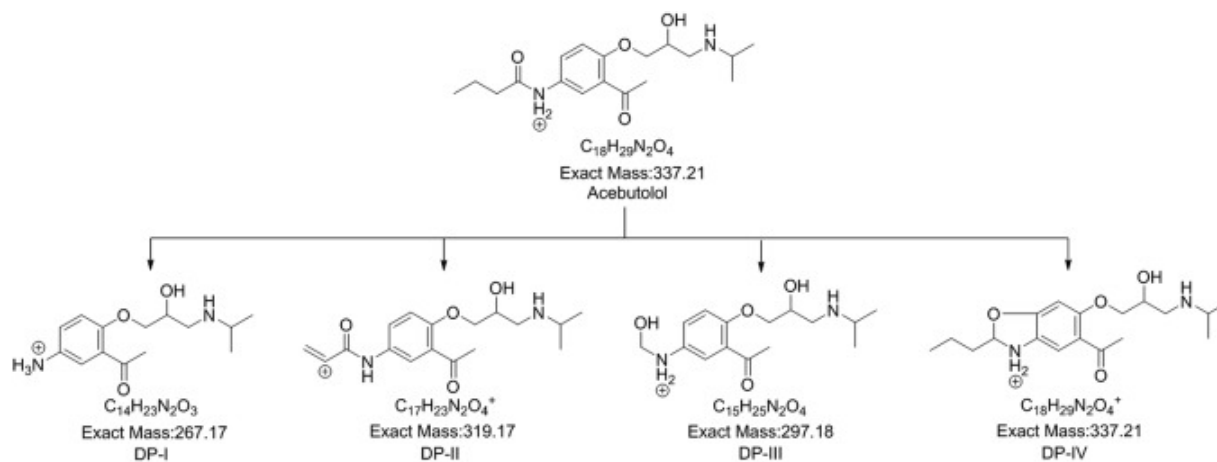
Download : Download high-res image (182KB)

Download : Download full-size image

Fig. 7. Degradation pathway of acebutolol.

3.7. In-silico carcinogenicity and hepatotoxicity

The carcinogenicity results obtained from TOPKAT, Lazar Toxicity and TOPKAT Extensible model software revealed that the drug (0.967) and DP-I (0.986) were found to be carcinogenic, while DP-II to DP-IV were non-carcinogenic. As per TOPKAT model assessment the values below 0.3 indicate non-carcinogen and above 0.7 signify carcinogen, while the values between 0.3 and 0.7 are considered in intermediate zone. All the compounds under investigation (acebutolol and its DPs) were found to be non-carcinogenic (inactive) as per Lazar Toxicity Prediction model and TOPKAT Extensible model. The results obtained in hepatotoxicity study by using Discovery Studio ADMET model revealed that the drug and all DPs were non-toxic. As per Discovery Studio ADMET, the computed probabilities for toxic and non-toxic values were 0.5 or more and 0.5 or less, respectively. But the results obtained for drug (0.490) and DP-IV (0.437) indicated high probability of hepatotoxic potential. The in-silico carcinogenicity and hepatotoxicity results are depicted in Table 5.

Table 5. In-silico carcinogenicity and hepatotoxicity study data of acebutolol and its DPs.

Drug/DPs	TOPKAT	Lazar toxicity	TOPKAT extensible	Discovery studio
Acebutolol	0.967 (carcinogen)	Inactive	0.435 (non-carcinogen)	0.490 (nontoxic)
DP-I	0.986 (carcinogen)	Inactive	0.514 (non-carcinogen)	0.397 (nontoxic)
DP-II	0.000 (non-carcinogen)	Inactive	0.000 (non-carcinogen)	0.000 (nontoxic)
DP-III	0.000 (non-carcinogen)	Inactive	0.000 (non-carcinogen)	0.000 (nontoxic)
DP-IV	0.000 (non-carcinogen)	Inactive	0.469 (non-carcinogen)	0.437 (nontoxic)

4. Conclusions

A forced degradation study on acebutolol was performed to determine its labile behaviour under respective stress condition. The drug was labile to acidic, alkaline and photolytic stresses, while it was stable in other neutral, oxidative and thermal conditions. The LC separation studies revealed the formation of four degradation products from the drug. DP-I was formed in acidic and basic conditions and DP-IV was generated only in basic condition. The two remaining minor DPs, DP-II and DP-III, were the products of photolytic degradation. The structures of all these degradants were resolved with the help of MS, MS^n, and LC–MS/MS analysis. The complete degradation pathway of the drug was established. The in-silico carcinogenicity study explored the carcinogenic potential of the drug and DP-I, while the values obtained by Discovery Studio software for the drug and DP-IV revealed a high probability of hepatotoxic potential.

Conflicts of interest

The authors declare that there are no conflicts of interest.

Special issue articles   Recommended articles

References

[1]   A.C. Moffat, M.D. Osselton, B. Widdop
        Clarke's Analysis of Drugs and Poisons
        Pharmaceutical Press, London (2005)
        : 569

        Google Scholar ↗

[2]   H. Jiang, C. Randlett, H. Junga, *et al.*
        Using supported liquid extraction together with cellobiohydrolase chiral stationary phases-based liquid chromatography with tandem mass spectrometry for enantioselective determination of acebutolol and its active metabolite diacetolol in spiked human plasma
        J. Chromatogr. B, 877 (2009), pp. 173-180

        📄 View PDF   View article   View in Scopus ↗   Google Scholar ↗

[3]   J. Szymura-Oleksiak, M. Walczak, J. Bojarski, *et al.*
        Enantioselective high performance liquid chromatographic assay of acebutolol and its active metabolite diacetolol in human serum
        Chirality, 11 (1999), pp. 267-271

        View in Scopus ↗   Google Scholar ↗

[4] R.B. Miller
A validated, high-performance liquid chromatographic method for the determination of acebutolol and diacetolol in human plasma
J. Liq. Chromatogr. Relat. Technol., 15 (1992), pp. 3233-3245

CrossRef ↗   Google Scholar ↗

[5] M. Piquette-Miller, R.T. Foster, F.M. Pasutto, *et al.*
Stereospecific high-performance liquid chromatographic assay of acebutolol in human plasma and urine
J. Chromatogr., 526 (1990), pp. 129-137

⬇ View PDF   View article   View in Scopus ↗   Google Scholar ↗

[6] M.G. Sankey, A. Gulaid, C.M. Kaye
Preliminary study of the disposition in man of acebutolol and its metabolites, diacetolol using a new stereoselective HPLC method
J. Pharm. Pharmacol., 36 (1984), pp. 276-277

View in Scopus ↗   Google Scholar ↗

[7] A.F. Al-Ghamdi, M.M. Hefnawy, A.A. Al-Majed, *et al.*
Development of square-wave adsorptive stripping voltammetric method for determination of acebutolol in pharmaceutical formulations and biological fluids
Chem. Cent. J., 6 (2012), pp. 1-8

CrossRef ↗   Google Scholar ↗

[8] S.A. Mostafavi, D.A. Stinson, K. Dooly, *et al.*
Excretion of acebutolol and its major metabolite diacetolol into infant blood circulation and the breast milk
Iran. J. Pharm. Res., 2 (2003), pp. 141-144

Google Scholar ↗

[9] M.S. Leloux, F. Dost
Doping analysis of beta-blocking drugs using high-performance liquid chromatography
Chromatographia, 32 (1991), pp. 429-435

View in Scopus ↗   Google Scholar ↗

[10] A. Tracqui, P. Kintz, P. Wendling, *et al.*
Toxicological findings in a fatal case of acebutolol self-poisoning
J. Anal. Toxicol., 16 (1992), pp. 398-400

CrossRef ↗   View in Scopus ↗   Google Scholar ↗

[11]   M.E. Abdel-Hamid
        Comparative LC–MS and HPLC analyses of selected antiepileptics and beta-blocking
        drugs
        Farmaco, 55 (2000), pp. 136-145
        ⬚ View PDF   View article   View in Scopus ↗   Google Scholar ↗

[12]   A. Levent
        Development of an ion-pair HPLC method for determination of acebutolol in
        pharmaceuticals
        Anal. Lett., 43 (2010), pp. 1448-1456
        CrossRef ↗   View in Scopus ↗   Google Scholar ↗

[13]   J. Krzek, A. Kwiecień, M. Żylewski
        Stability of atenolol, acebutolol and propranolol in acidic environment depending
        on its diversified polarity
        Pharm. Dev. Technol., 11 (2006), pp. 409-416
        CrossRef ↗   View in Scopus ↗   Google Scholar ↗

[14]   A. El-Gindy, A. Ashour, L. Abel-Fattah, et al.
        First derivative spectrophotometric, TLC-densitometric, and HPLC determination of
        acebutolol HCL in presence of its acid-induced degradation product
        J. Pharm. Biomed. Anal., 24 (2001), pp. 527-534
        ⬚ View PDF   View article   View in Scopus ↗   Google Scholar ↗

[15]   M. Ogrodowczyk, K. Dettlaff, P. Kachlicki, et al.
        Identification of radiodegradation product of acebutolol and alprenolol by HPLC/
        MS/MS
        J. AOAC Int., 98 (2015), pp. 46-50
        CrossRef ↗   View in Scopus ↗   Google Scholar ↗

[16]   ICH Q1A(R2) Guideline: Stability testing of new drug substances and products (2003)
        International Conference on Harmonisation (ICH), IFMPA, Geneva, Switzerland.
        Google Scholar ↗

[17]   ICH Q1B Guideline: Stability testing: Photostability testing of new drug substances and
        products International Conference on Harmonisation (ICH), IFPMA, Geneva, Switzerland,
        1996.
        Google Scholar ↗

[18]   ICH Q2(R1) Guideline: Validation of Analytical Procedures: Text and Methodology
        International Conference on Harmonization (ICH), IFPMA, Geneva, Switzerland, 2005.

Google Scholar ↗

[19]   P. Szymański, M. Markowicz, E. Mikiciuk-Olasik

Adaptation of high-throughput screening in drug discovery-toxicological screening test

Int. J. Mol. Sci., 13 (2012), pp. 427-452

View in Scopus ↗   Google Scholar ↗

Cited by (16)

Disposable cerium oxide/graphene nanosheets based sensor for monitoring acebutolol in environmental samples and bio-fluids

2022, Journal of Environmental Chemical Engineering

Citation Excerpt :

…The residues of ACT and the effluents from waste water treatment stand as a huge hindrance in reducing environmental pollution [7]. The higher intake of ACT is able to cause several side effects and one among them is drug induced lupus erythematosus which occurs due to cutaneous eruptions with the antinuclear antibodies produced in plasma [8,9]. Significant insights are being reported and explored for ACT detection with several modern techniques [10].…

Show abstract ⌄

Modeling and regulation of neonicotinoid insecticides exposure in agricultural planting areas for reducing the human health risks

2021, Journal of Cleaner Production

Citation Excerpt :

…TOPKAT is an effective tool that can provide abundant toxicity information. For example, Rakibe et al. (2018) used TOPKAT to predict the carcinogenicity of acebutolol's by-products. In addition, the human health risk integrated assessment (HHRIA) index and grade of neonics were characterized using the CIW method.…

Show abstract ⌄

Functional modification of HHCB: Strategy for obtaining environmentally friendly derivatives

2021, Journal of Hazardous Materials

Citation Excerpt :

…In this study, the toxicokinetic simulation and molecular docking was employed to investigate human health

risk of the designed SMs' derivatives. The toxicokinetic simulation calculation procedures were performed using TOPKAT Extensible module (Blessy Christina et al., 2012; Rakibe et al., 2018), in Discovery Studio® 2020 software. The predicted toxicokinetic parameters of HHCB before and after modification are shown in Tables 4, 5 and 6....

Show abstract ∨

Identification of the chemical components and metabolites of tripterygium glycoside tablets in mice by HPLC-Q/TOF MS

2019, Journal of Chromatography B: Analytical Technologies in the Biomedical and Life Sciences

Citation Excerpt :

…It's a common structure-toxicity model that has been widely used in toxicity prediction [25,29–31]. The model was developed from available literature data of 382 compounds known to exhibit liver toxicity or trigger dose-related elevated aminotransferase levels in >10% of the human population [29]. All possible structures of the metabolites were included if the biotransformation sites were uncertain....

Show abstract ∨

Further exploration of the collision-induced dissociation of select beta blockers: Acebutolol, atenolol, bisoprolol, carteolol, and labetalol ↗

2023, Journal of Mass Spectrometry

Forced Degradation Study of Zanubrutinib: An LC-PDA and LC-MS Approach ↗

2022, Journal of Chromatographic Science

> View all citing articles on Scopus ↗

Peer review under responsibility of Xi'an Jiaotong University.